Analysis of Neuron–Specific enolase isozymes in human serum using immunoaffinity purification and liquid chromatography–tandem mass spectrometry quantification

Journal of Chromatography B 1223 (2023) 123701

Contents lists available at ScienceDirect

Journal of Chromatography B

journal homepage: www.elsevier.com/locate/jchromb

Analysis of Neuron–Specific enolase isozymes in human serum using immunoaffinity purification and liquid chromatography–tandem mass spectrometry quantification

Sylvia A.A.M. Genet [a,b,d], Jur R.E. Wolfs [a], Chris B.A.K. Vu [a], Madita Wolter [a], Maarten A. C. Broeren [c,d], Joost van Dongen [a,d], Luc Brunsveld [a,d], Volkher Scharnhorst [a,b,d], Daan van de Kerkhof [a,b,d,*]

[a] Laboratory of Chemical Biology, Department of Biomedical Engineering and Institute for Complex Molecular Systems, Eindhoven University of Technology, Eindhoven, the Netherlands
[b] Catharina Hospital Eindhoven, Eindhoven, the Netherlands
[c] Máxima Medical Center, Eindhoven/Veldhoven, the Netherlands
[d] Expert Center Clinical Chemistry Eindhoven, Eindhoven, the Netherlands

ARTICLE INFO

Keywords:
Neuron–specific enolase (NSE)
Reversible protein denaturation
Lung cancer
immunoaffinity (IA)
Tryptic digestion
Liquid chromatography–tandem mass spectrometry (LC–MS/MS)

ABSTRACT

Neuron–specific enolase (NSE) is a promising small–cell lung cancer (SCLC) biomarker composed of αγ and γγ isozyme dimers. As the conventional immunoassays are prone to interferences and cannot differentiate between the isozymes, we developed a multiplex immunoaffinity (IA) liquid chromatography–tandem mass spectrometry (LC–MS/MS) assay for the quantification of NSEα and NSEγ in human serum. A calibrator was prepared by performing cold denaturation of recombinantly expressed αα and γγ enolase dimers to induce a new dimer equilibrium that was determined to be approximately 1αγ:1γγ:1αα. Selective sample purification was achieved by performing IA extraction using an antibody specific towards NSEγ. The isolated αγ and γγ dimers were denatured and trypsin digested to allow quantification of the selected signature peptides and their corresponding isotopically labelled peptide internal standard. The obtained linear dynamic ranges were determined to be 1.5–56 ng/mL and 0.64–167 ng/mL for NSEα and NSEγ (R^2 = 0.88 and 0.97 respectively). Validation of the assay showed acceptable accuracy and precision for NSEα and NSEγ. The method was successfully applied to patient serum in which both isozymes were detected. Compared to the conventional immunoassay, substantially lower total NSE concentrations were measured in IA LC–MS/MS. With this multiplex IA LC-MS/MS assay, the clinical value of quantifying the individual isozymes can be explored. In addition, together with the calibrator described here, it may be applied to standardize NSE immunoassays across different platforms.

1. Introduction

Neuron–specific enolase (NSE) is a glycolytic metalloenzyme that is composed of αγ and γγ dimers and was originally discovered in the extracts of brain tissue [1,2]. NSE is part of the enolase family, which comprises three enolase isozymes, forming five dimeric combinations: αα, αβ, ββ, αγ and γγ [3–5]. The αγ and γγ dimers are predominantly expressed in neurons and neuroendocrine cells, including neuroendocrine tumors like small–cell lung cancer (SCLC). The αγ heterodimer and low concentrations of the γγ homodimer are also found in erythrocytes and platelets [6,7].

In recent years, NSE has been reported to be a promising tumor marker for the diagnosis and follow–up of SCLC, as elevated serum NSE concentrations correlated with disease progression [6]. Improved diagnostic value was observed by combining NSE detection with the assessment of other protein tumor markers such as cytokeratin fragment 21–1 [8–12]. Nevertheless, the clinical applicability of NSE quantification using the traditional sandwich immunoassays is hampered by the lack of concordance between assays and the falsely elevated concentrations caused by hemolysis [13–16]. Above all, the inability to separately quantify the αγ and γγ dimers limits the opportunity to investigate their individual added value in lung cancer diagnostics.

* Corresponding author at: Clinical Laboratory Catharina Hospital Eindhoven, Michelangelolaan 2, 5623 EJ Eindhoven, The Netherlands.
E-mail address: daan.vd.kerkhof@catharinaziekenhuis.nl (D. van de Kerkhof).

https://doi.org/10.1016/j.jchromb.2023.123701
Received 25 January 2023; Received in revised form 29 March 2023; Accepted 3 April 2023
Available online 13 April 2023

Immunoaffinity-liquid chromatography–tandem mass spectrometry (IA LC–MS/MS) is a relatively new approach that has confirmed its potential in clinical diagnostics [17]. This hybrid method combines elements of a ligand binding assay and MS, therewith ensuring maximum selectivity enabling protein quantification in complex matrices in the low ng/mL range. The number of IA LC–MS/MS methods for peptide and protein biomarker quantification significantly increased during the past decade [17], including thyroglobulin [18] and parathyroid hormone-related peptide [19] assays, which are now used by laboratories in clinical practice. LC–MS/MS approaches pose multiple advantages compared to immunoassays alone, as they offer the opportunity to quantify multiple biomarkers in a single run (multiplexing) and to obtain additional molecular information such as isoform differentiation and identification of post–translational modification. An example of this is prostate–specific antigen, where quantification of its isoforms was shown to improve the specificity of prostate cancer diagnostics [20]. Likewise, a NSEγ quantification approach based on IA LC–MS/MS was described by Torsetnes et al., showing potential for the quantification of NSE in a multiplex format, although quantitative analysis of the NSEα isoform was not achieved due to the lack of commercially available NSEαγ calibrators [21,22]. There is thus need to develop NSEαγ calibrators that could support the quantitative analysis of the two NSE isoforms simultaneously using IA LC–MS/MS.

In this study, NSEαγ heterodimers were formed *via* reversible dissociation using cold denaturation of recombinantly expressed NSEα and NSEγ. The obtained calibrator was used to confirm successful and selective purification, separation and quantification of NSEαγ and NSEγγ in a newly developed multiplex IA LC–MS/MS assay. The applicability of the method in patient samples and correlation with a conventional immunoassay were shown. The standards and multiplex IA LC–MS/MS assay therefore set the foundation to further study the role of the different NSE isozymes in lung cancer diagnostics.

2. Experimental

2.1. Chemicals and reagents

Stable isotopically labeled internal standard (IS) peptides ELPLY[R_$^{13}C_6$_$^{15}N_4$] (99.9% purity) and TIAPALVS[K_$^{13}C_6$_$^{15}N_2$] (95% purity) were obtained from Pepscan BV (Lelystad, The Netherlands), diluted in MilliQ (MQ) with 10% acetonitrile (ACN) and 0.1% formic acid (FA) and stored in aliquots at −80 °C.

Anti–h NSE 9601 SPTN-5 monoclonal mouse antibody was obtained from Medix Biochemica (Espoo, Finland). Protein G Dynabeads and BS $(PEG)_5$ were purchased from Thermo Fisher Scientific (Waltham, MA, USA). Sequencing grade modified trypsin was purchased from Promega (Madison, WI, USA), diluted in 50 mM acetic acid to a concentration of 30 ng/μL, aliquoted and stored at −80 °C. LC-MS grade mobile phase solvents were obtained from Biosolve (Valkenswaard, The Netherlands). 14–3-3 Tobacco was kindly supplied by Thijs van Veldhuisen (Eindhoven University of Technology, The Netherlands). Adult bovine serum and all other reagents were purchased from Sigma-Aldrich (Saint Louis, MO, USA).

2.2. Protein expression

His-tagged NSEα and NSEγ were expressed in *E. coli* BL21 (DE3) cells with a pET28a(+) plasmid (Genscript Biotech, Leiden, The Netherlands) and pJL-*H*10-ENO2 plasmid (MD Anderson Cancer Center, Houston, TX), respectively. Both proteins were purified following standard procedures using nickel column purification and size exclusion chromatography. Sequence identity and purity was confirmed using high resolution (HR) Q–TOF LC-MS and sodium dodecyl sulfate–polyacrylamide gel electrophoresis (Supplementary Fig. 1 &2). Purified proteins were dissolved in 20 mM Tris-HCl pH 7.4, 150 mM NaCl, 0.5 mM TCEP and stored at −80 °C until use.

2.3. Signature peptide selection

Signature peptide (SP) selection was performed by evaluating the tryptic peptides of NSEα and NSEγ based on the uniqueness in the human genome using BlastP software (https://blast.ncbi.nlm.nih.gov/Blast.cgi), number of amino acids ($6 < n < 25$), the presence of potentially unstable amino acids (M, C, N, Q), signal intensity and chromatographic interference. The latter was evaluated by separately dissolving 5 μg of NSEα and NSEγ in 50 mM Tris-HCl + 1 mM $CaCl_2$ pH 7.6 followed by denaturation at 95 °C at 1200 rpm for 10 min and overnight digestion at 37 °C and 600 rpm using a 1:20 trypsin:protein ratio (w/w). The reaction was stopped by adding 2% formic acid (FA). Samples were then analyzed using HR Q–TOF-LC–MS[e] (Waters, Milford, MA) to confirm the sequence identity of the precursor and product ions. This is a data acquisition mode that alternates low-energy and high-energy collision energies (CE), enabling the measurement of precursor and product-ions within one chromatographic run.

2.4. Antibody coupling to protein G functionalized magnetic beads

The coupling procedure was performed multiple times using LoBind Eppendorf/Falcon tubes, according to the following general procedure: 8.33 μL protein G Dynabeads were washed twice in 250 μL conjugation buffer (100 mM sodium phosphate, 70 mM NaCl, 0.05% Tween–20 (v/v), pH 8.0). The supernatant was removed and 250 μL of 8 μg/mL Anti-h NSE 9601 dissolved in conjugation buffer was added to the beads. After 30 min incubation with rotation, 1.25 μL of 5 mM $BS(PEG)_5$ dissolved in cold conjugation buffer was added (final concentration 25 μM) and incubated for 30 min with rotation. The reaction was quenched by adding 25 μL of 1 M Tris–HCl, pH 7.5 for 15 min with rotation. The supernatant was removed and unbound antibody was eluted by adding 50 μL (elution 1) and 200 μL (elution 2) elution buffer (1 M NaSCN in 100 mM Tris–HCl, pH 7.5) for 5 min with rotation. The beads were then washed twice with 250 μL PBS, 0.1% Tween–20, pH 7.4 and subsequently stored in this buffer at 4 °C until further use. For large–scale experiments, volumes were multiplied by the number of equivalents.

2.5. Immunoaffinity extraction of NSE

For all samples described in this study, either dissolved in 5% BSA in PBS or in different types of serum, 250 μL of the Anti–h NSE 9601 coated magnetic beads was transferred into a LoBind Eppendorf tube and the supernatant was removed. The beads were washed twice with 200 μL PBS 0.1% Tween–20, pH 7.4 after which the supernatant was removed and 1 mL sample was added to the beads. Samples were incubated for 2 h at room temperature with rotation and after removal of the supernatant, the beads were successively washed two times with 200 μL PBS 0.1% Tween–20, pH 7.4 and two times with 200 μL PBS, pH 7.4. The beads were then resuspended in 80 μL digestion buffer (50 mM Tris-HCl, 1 mM $CaCl_2$, pH 8.0) containing 0.46 ng TIAPALVS[K_$^{13}C_6$, $^{15}N_2$] and 0.42 ng ELPLY[R_$^{13}C_6$, $^{15}N_4$].

2.6. Tryptic digestion

The sample was denatured for 10 min at 95 °C and 1200 rpm after which the mixture was cooled down and shortly centrifuged. Digestion was initiated by incubating with 300 ng trypsin for 2 h at 37 °C and 1200 rpm. To stop the reaction, the sample was put on ice and a mixture of ACN and FA (final composition 10% ACN, 2% FA) was added. The supernatant was transferred to a new LoBind Eppendorf tube, centrifuged for 10 min at 13400 rpm and transferred into a LC–MS vial.

2.7. Instrumentation and chromatographic conditions

Analysis of the recombinantly expressed proteins and evaluation of potential SPs were performed using a Xevo G2 HR Q–TOF coupled to an

Table 1
Optimized MRM transitions for the NSEα and NSEγ SPs (TIAPALVSK: $450.28^{2+}>685.45^{+}$ and $450.28^{2+}>614.40^{+}$, ELPLYR: $395.72^{2+}>274.75^{2+}$ and $395.72^{2+}>548.35^{+}$ respectively) and their corresponding IS (TIAPALVS[K_$^{13}C_6$, $^{15}N_2$]: $454.28^{2+}>693.45^{+}$, ELPLY[R_$^{13}C_6$, $^{15}N_4$]: $400.73^{2+}>279.80^{2+}$). MRM: multiple reaction monitoring, SP: signature peptide, IS: internal standard, CE: collision energy.

Protein	Peptide sequence	Precursor (*m/z*)	Product (*m/z*)	Product ion type	Q1 pre-bias (V)	CE (V)	Q3 pre-bias (V)
NSEα	TIAPALVSK (quantifier, SP)	450.28	685.45	$y7^{+}$	−13	−14	−28
	TIAPALVSK (qualifier, SP)	450.28	614.40	$y6^{+}$	−13	−15	−24
	TIAPALVS[K_$^{13}C_6$, $^{15}N_2$], (IS)	454.28	693.45	$y7^{+}$	−13	−14	−28
NSEγ	ELPLYR (quantifier, SP)	395.72	274.75	$y4^{2+}$	−20	−13	−21
	ELPLYR (qualifier, SP)	395.72	548.35	$y4^{+}$	−20	−14	–22
	ELPLY[R_$^{13}C_6$, $^{15}N_4$], (IS)	400.73	279.80	$y4^{2+}$	−20	−14	–22

Acquity UPLC I class binary solvent manager and Acuity UPLC Sample Manager-FL (Waters, Milford, MA). An Agilent Polaris C8–A (2.0x150mm, 3 μm) column was used for chromatographic separation with a flow of 0.3 mL/min and a column temperature of 60 °C. The mobile phases consisted of (A) 0.1% FA in MQ and (B) 0.1% FA in ACN. The gradient in minutes per percentage of mobile phase B was 0.0 min/15%, 7.5/75, 8.0/75, 8.1/15 and 10/15. The tryptic peptides were evaluated with the same conditions using an Agilent Polaris C18-A (2.0x100 mm, 3 μm) column and a gradient in minutes per percentage of mobile phase B of 0.0 min/5%, 23.5/80, 23.6/90, 25.0/90, 25.1/5 and 30/5. Electrospray ionization (ESI) was operated in positive mode. In case of the tryptic peptide evaluation, mass spectra were collected in MS^e mode with a ramped CE from 20 to 50 V over the range of 100–2000 *m/z*. Peptide sequencing was performed using the BioLynx application within the software (Waters, Milford, MA).

Quantitative analysis was done on a LCMS–8045 triple quadrupole coupled to a Nexera–I LC–2040C 3D Plus (Shimadzu, Kyoto, Japan) and Shimadzu LabSolutions software (version 5.93). Chromatographic separation was carried out using an Agilent Polaris C18-A (2.0x100 mm, 3 μm) column with a gradient of 0.0 min/5%, 11.0/20, 15.3/80, 15.5/90, 16.0/90, 16.1/5 and 21/5. The flow was directed to waste the first 8.6 min and after 9.5 min. The flow rate was set to 0.3 mL/min, the column temperature to 50 °C and the sample temperature to 15 °C. The injection volume was determined to be 15 μL. The ESI was operated in positive mode with the optimized transition settings of the SP and IS listed in Table 1. The TIAPALVSK transitions were measured from 8.6 until 9.1 min and the ELPLYR transitions were measured from 9.0 until 9.5 min.

2.8. Preparation of NSE depleted serum

Whole blood of 10 healthy volunteers was collected in 8.5 mL BD Vacutainer SSTII Advance Plus Blood Collection Tubes during routine venipuncture. The sera were obtained within one hour after collection by centrifugation for 10 min at 2683 g at 20 °C and subsequently pooled. Depletion of NSE was performed in 6 incubation steps using the magnetic bead constructs and 1 mL sample volume. After incubation, the supernatant was collected and the captured NSE was eluted using 1 M NaSCN. The beads were re-equilibrated prior to renewed addition of the supernatant. The remaining NSE concentration was checked 4 times using the bottom-up LC-MS/MS procedure described above.

2.9. Heterodimerization

To confirm spontaneous homodimerization of self-expressed NSEα and NSEγ, Dynamic Light Scattering (DLS) was performed using 14–3-3 Tobacco as a reference protein. NSEα, NSEγ and 14–3-3 Tobacco were each dissolved at 16.2 μM in 10 mM Tris-HCl, 150 mM NaCl at pH 7.4 and filtered using a Whatman 0.2 μm syringe filter. A Malvern instrument Zetasizer (model Nano ZSP) and Zetasizer software were used to analyze and process the data. DLS measurements were conducted at 25 °C with 100 μL sample volume.

NSE heterodimerization was assessed by spiking solutions of 100 and 200 μg/mL NSEα and NSEγ in PBS. The samples were individually snap frozen and stored at −70 °C for 2 days to achieve heterodimerization. The samples were then diluted in native loading buffer (62.5 mM Tris-HCl, pH 6.8 [40% (v/v) glycerol, 0.01% (w/v) bromophenol blue]). Native polyacrylamide gel electrophoresis (PAGE) was performed by loading 1 and 2 μg protein of the 100 and 200 μg/mL samples respectively (n = 2) into pre-casted polyacrylamide gels (Bio-Rad Laboratories, Hercules, CA USA), which were submerged in native running buffer (25 mM Tris-HCl, 192 mM glycine, pH 8.3). The gels were ran for 160 min at 100 V at 4 °C, stained using Coomassie G250 staining for 30 min and destained in MilliQ overnight.

In gel digestion was performed by adding 100 mM ammonium bicarbonate/ACN (1:1, v/v) to gel pieces followed by incubation for 30 min. Neat ACN was added and the samples were incubated at room temperature until the gel pieces became colorless and shrunk. The dry gel pieces were submerged in trypsin buffer (7.5 ng/μL trypsin, 50 mM ammonium bicarbonate [10% (v/v) ACN]) and incubated for 2 h at 4 °C. Digestion was performed in a thermomixer at 37 °C and 1200 rpm overnight. Extraction of the digest was facilitated by addition of 100 μL extraction buffer (5% FA / ACN [1:2, v/v]) and subsequent incubation at 37 °C for 15 min. The digest was collected after addition of 20 μL MilliQ (0.1% [v/v] FA).

2.10. Assay validation

The NSE calibrator was made by adding 100 μg/mL NSEα and 100 μg/mL NSEγ to PBS, which was then stored for 2 days at −70 °C. Calibration standards were prepared in NSE depleted serum (NDS) by serial dilutions starting with 500 ng/mL and subsequently stored at –70 °C. Calibration curves were constructed using a sample volume of 1.0 mL (n = 3, at 2 different days). Background subtraction was applied. For each analytical run, peak area ratios of the SP and IS were plotted versus the nominal concentrations of the calibration standards using linear least–squares regression with a weighing factor of $1/x^2$. The lower limit of quantification (LLoQ) was calculated using the formula: 10•(standard error of y–intercept/slope). The regression equation of the calibration curve was used to back–calculate the measured concentrations for the standards and the results were compared to nominal concentrations to obtain accuracy, expressed as a percent deviation (%) from the nominal value, and precision, expressed as coefficient of variation (CV, %). The results were compared to European Medicines Agency (EMA) guidelines, which recommend acceptance criteria of < 15% and < 20% for chromatographic methods and ligand binding assays respectively and < 20% and < 25% for LLoQ thereof. Carry-over was assessed by measuring blank samples after the highest calibration standard. Specificity towards NSEαγ and NSEγγ was evaluated by comparing the peak area ratio of blank samples to samples containing 25 ng/mL NSEα (in the absence of NSEγ).

2.11. Comparative study

Residual serum samples were pooled to obtain nine independent serum pools. A commercially available electrochemiluminescent assay (ECLIA) was used for the quantification of NSE. The test was validated and performed on a Cobas platform (e801, Roche Diagnostics, Rotkreuz, Switzerland).

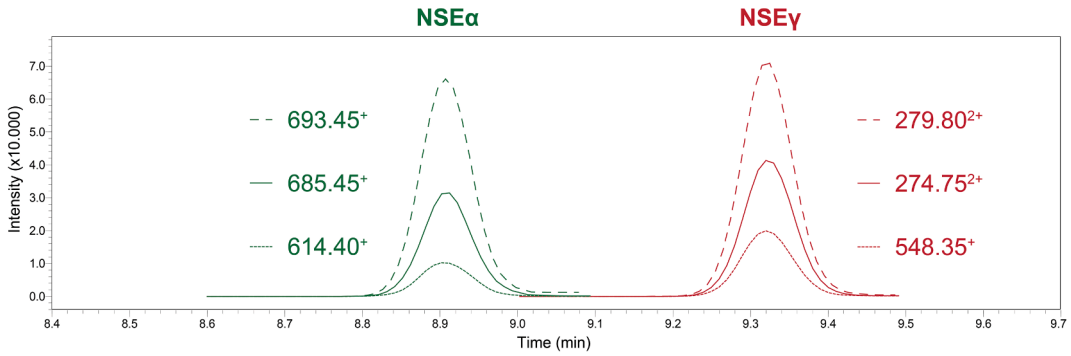

Fig. 1. MRM chromatogram of the NSEα and NSEγ SPs (TIAPALVSK: 450.28^{2+}>685.45^{+} and 450.28^{2+}>614.40^{+}, ELPLYR: 395.72^{2+}>274.75^{2+} and 395.72^{2+}>548.35^{+} respectively) and their corresponding IS (TIAPALVS[K_$^{13}C_6$, $^{15}N_2$]: 454.28^{2+}>693.45^{+}, ELPLY[R_$^{13}C_6$, $^{15}N_4$]: 400.73^{2+}>279.80^{2+}). MRM: multiple reaction monitoring, SP: signature peptide, IS: internal standard.

2.12. Study design and participants

Clinical samples of lung cancer patients were pooled and used for assay comparison. The samples were selected from a clinical study (lung marker study NL9146, ICTRP Search Portal (who.int)) described elsewhere [16,23–25], ethically approved by the Medical Research Ethics Committees United (NL58985.100.16).

3. Results and discussion

3.1. Signature peptide selection

The tryptic peptides of recombinantly expressed NSEα and NSEγ were assessed based on their uniqueness in the human genome, peptide length, the absence of unstable amino acids and detectability. The previously described [21] TIAPALVSK (NSEα) and ELPLYR (NSEγ) peptides met all criteria (Supplementary Fig. 3) and were therefore selected as SPs for their respective isozymes. Corresponding stable isotopically labeled peptides TIAPALVS[K_$^{13}C_6$, $^{15}N_2$] and ELPLY[R_$^{13}C_6$, $^{15}N_4$] were chosen as IS to correct for experimental variation after tryptic digestion. Multiple reaction monitoring (MRM) optimization resulted in optimized transitions and CE for all peptides (Table 1). The qualifier/quantifier ratio was used for quality control. To obtain good chromatographic separation of the two SPs, a gentle gradient for the separation and elution of both SPs was used, a subsequent steeper gradient for the elution of remaining substances followed by an equilibration phase to prepare the column for the next run. The final LC method yielded suitable values for the retention factor ($k \geq 3$) and chromatographic resolution ($R_s \geq 1.5$) and both SPs co–eluted with their corresponding IS (Fig. 1).

3.2. Immunoaffinity purification using protein G functionalized magnetic beads

Preanalytical sample purification was performed using an IA purification step with Anti–h NSE 9601, which is described to be a high affinity antibody towards NSEαγ and NSEγγ without cross–reactivity with αα–homodimers [26]. The antibody was covalently coupled to protein G functionalized magnetic beads using a $BS(PEG)_5$ linker [27]. First, assay conditions including the antibody–bead–linker concentration, incubation time, digestion time (Supplementary Fig. 4A) and number of washing steps were optimized, revealing no significant differences between the optimal isolation conditions of NSEγ and NSEα (data not shown). Due to the presence of endogenous NSE in human serum, the use of surrogate matrices was investigated for calibration and validation purposes. A 5% BSA solution appeared to be insufficient as a surrogate matrix, as the peak area ratio significantly increased compared to bovine serum and diluted samples thereof (illustrated for NSEγ in

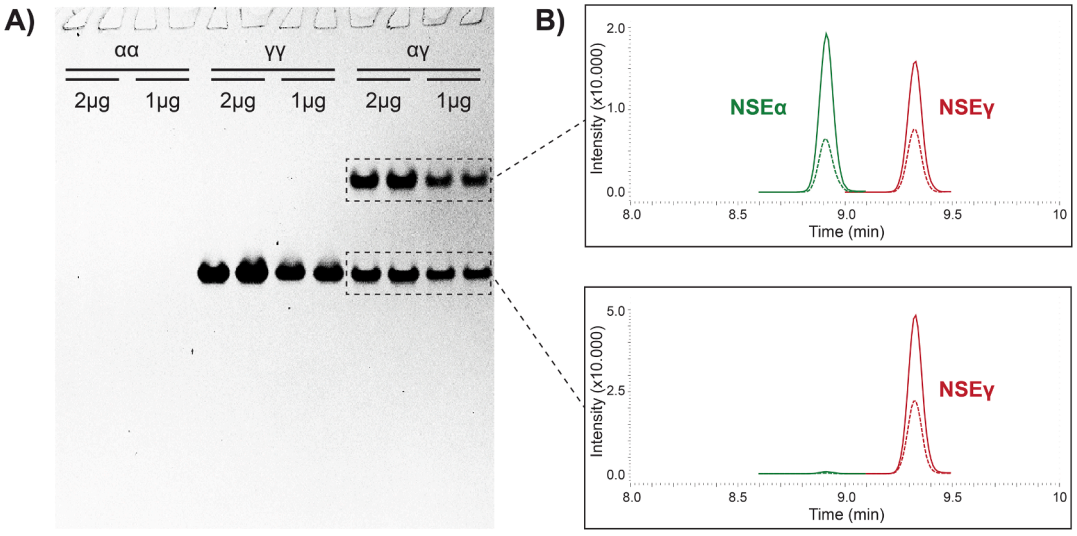

Fig. 2. Formation of NSEαγ heterodimers. A) Native PAGE of αα, γγ and the freeze–thawed αγ samples, revealing an additional αγ band in the freeze–thawed αγ samples compared to γγ solely. No band was seen in case of αα as is was not negatively charged and therefore not attracted towards the positive pole. B) In gel digestion and LC–MS/MS quantification of the two bands appearing in the NSEαγ samples, showing an NSEγ signal for the lower band and an NSEα and NSEγ signal for the upper band. PAGE: polyacrylamide gel electrophoresis.

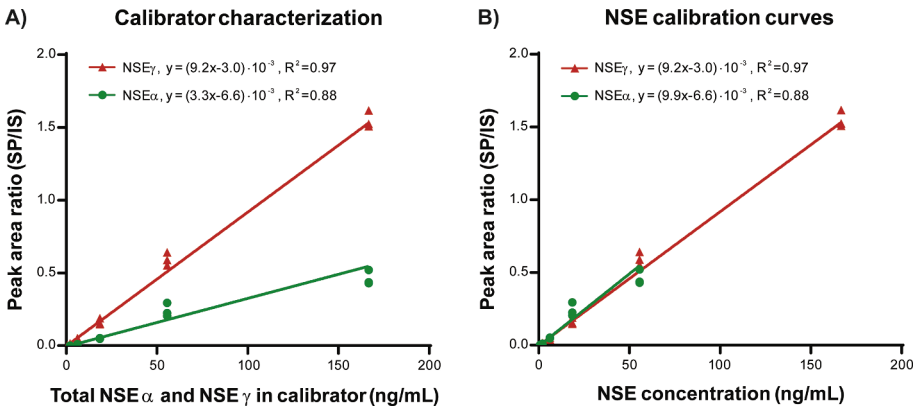

Fig. 3. Characterization and calibration using the NSE calibrator (NSEα: green dots, NSEγ: red triangles). A) Spiking of the calibrator in NDS revealed a NSEα:NSEγ slope ratio of 0.36, indicating a 1:3 NSEα:NSEγ ratio. B) Constructed calibration curves after correction of the NSEα concentration by dividing the NSEα concentration by 3 based on the 1:1:1 ratio of αγ:γγ:αα (n = 3, 2 days). NDS: NSE depleted serum, SP: signature peptide, IS: internal standard. (For interpretation of the references to colour in this figure legend, the reader is referred to the web version of this article.)

Supplementary Fig. 4B), which is a known phenomenon most probably caused by non–specific binding of other serum proteins [28]. To obtain a surrogate matrix, NSE depleted serum (NDS) was made by performing multiple NSE depletion cycles in pooled human serum using the antibody–bead constructs until the signal stagnated, resulting in minor background NSE signal that was subtracted from the overall signal (Supplementary Fig. 5).

3.3. NSEα and NSEγ heterodimerization

Enolases are dimeric in structure, where γγ is known to have the highest binding affinity (15 nM), αα is the least stable and the heterodimer has intermediate stability [29,30]. DLS was performed to confirm that the expressed αα and γγ enolases were present in a dimeric state (Supplementary Fig. 6). The experiments on αα and γγ enolase showed hydrodynamic diameters of 7.2 ± 2.0 nm and 5.9 ± 1.6 nm respectively. This theoretically corresponds to a spherical particle/protein of around 210 ± 106 kDa and 106 ± 46 kDa respectively, which is in line with the calculated masses of ~ 97 kDa of the dimers. The mass calculations were based on a spherical model, which is not expected to match the actual shape of the protein dimers exactly. The well–known homodimeric protein 14–3-3 Tobacco (~58 kDa in dimeric state) was used as a reference, showing comparable results.

Previous studies showed that reversible dissociation techniques including pressure–, temperature– and salt induced denaturation resulted in successful dissociation of the homodimers and formation of the NSEαγ heterodimer. It was assumed that the recombinantly expressed proteins were also present as homodimers and so several reversible dissociation techniques were evaluated *via* native polyacrylamide gel electrophoresis (PAGE). As shown in Fig. 2A, a single band was visible for a sample containing NSEγγ solely, whereas no protein band was visible for a sample containing αα enolase alone. The absence of a band in case of αα could be explained by the large difference in isoelectric point of 7.38 (γ) and 4.75 (α) [31]. Consequently, γγ carries a net negative charge while αα does not, resulting in stronger attraction of γγ towards the positive pole, while αα will not be attracted. Neither incubation of a 1:1 equimolar ratio of α:γ in PBS at room temperature nor heat (40 °C) or salt (KBr) induced denaturation resulted in successful heterodimerization (data not shown). However, incubation of a 1:1 ratio of α:γ in PBS followed by a freeze–thaw cycle did result in an additional protein band compared to the individual γγ homodimer (Fig. 2A). This dissociation technique is called cold denaturation and has previously been applied for reversible dissociation of other protein complexes [32–34]. In–gel digestion revealed a NSEγ signal for the lower protein band and a NSEα and NSEγ signal for the new upper band, which confirms the successful heterodimerization (Fig. 2B). Comparable intensities of the NSEαγ and NSEγγ protein bands in both the 1 and 2 μg samples demonstrates a roughly 1:1 ratio of both dimers and therewith a final composition of roughly 1αγ:1γγ:1αα. The mixture of homo– and heterodimers was used as calibrator in further quantitative experiments.

3.4. Further characterization of the calibrator

To allow for the use of the heterodimerized NSE calibrator for validation of the IA LC–MS/MS assay, the exact dimer composition should be quantified. To this end, the signals obtained after performing the IA LC–MS/MS assay were compared to direct digestion of the calibrator without performing IA purification. During direct digestion, all dimeric isozymes in the mixture are digested including αα enolase, while this homodimer is not detected during IA purification as only NSE dimers containing the γ isozyme are captured by the antibody. Therefore, direct digestion of the standard containing equimolar amounts of NSEα and NSEγ will represent the maximum NSEα:NSEγ peak area ratio that can be obtained when performing the IA LC–MS/MS assay with a sample that contains the NSEαγ heterodimer solely. The NSEα:NSEγ peak area ratio (SP/IS of NSEα divided by SP/IS of NSEγ) in direct digestion was determined to be 1.08 ± 0.15 (mean + standard deviation). If the NSEα signal obtained after performing IA LC–MS/MS is lower, and therefore also the NSEα:NSEγ peak area ratio, it is expected that the calibrator is composed of the αγ heterodimer and γγ and αα homodimers. To confirm this, increasing concentrations of the calibrator were spiked in NDS and measured using the IA LC–MS/MS assay (Fig. 3A). By dividing the slope of NSEα by the slope of NSEγ, the NSEα:NSEγ peak area ratio was calculated to be 0.36. Compared to the peak area ratio of 1.08 in case of direct digestion, this indicates a ratio of approximately 1NSEα:3NSEγ. This implies an overall 1:1:1 M ratio of αγ:γγ:αα dimers in the calibrator, which is confirmed by the native PAGE results (Fig. 2A).

3.5. Assay validation

During IA purification, only αγ and γγ are captured by the antibody, while the irrelevant αα dimer is not isolated. To this end, a NSEγ calibration curve can be constructed by plotting the spiked NSEγ concentration in the calibrator against the detected signal, while the total NSEα concentration in the calibrator should be divided by 3 to construct a NSEα calibration curve, as the dimer ratio (1αγ:1γγ:1αα) indicates that only 1 out of 3 α monomers is detected during the IA LC–MS/MS assay, i.e. the NSEα monomers in the αγ heterodimer. As shown in Fig. 3B, linearity was achieved for both NSEα and NSEγ (R^2 = 0.88 and 0.97 respectively) up to a NSEγ concentration of 167 ng/mL respectively, above which curve flattening was observed caused by saturation of the beads. The LLoQ of NSEα and NSEγ were calculated to be 1.5 ng/mL and 0.64 ng/mL respectively and so final detection ranges of 1.5–56 ng/mL for NSEα and 0.64–167 ng/mL for NSEγ were achieved. Until to date, no differentiation between both isozymes in healthy nor SCLC patients has been established. As such, the exact relevant concentration range for both isozymes is unknown. Notwithstanding, we previously reported total serum NSE concentrations ranging from 4.59 to 370 ng/mL

Table 2
Statistics of the back–calculated concentrations of the isozyme calibration curves analyzed over two days (n = 3).

NSEα	Concentration (ng/mL)	56	19	6.2	2.1	0.69	
	Mean accuracy (% bias)	−15	34	−6.5	19	5.8	N.A.
	Mean precision (% CV)	11	19	5.7	11	46	N.A.
NSEγ	**Concentration (ng/mL)**	**167**	**56**	**19**	**6.2**	**2.1**	**0.69**
	Mean accuracy (% bias)	1.2	17	−2.4	−10	−9.7	4.2
	Mean precision (% CV)	3.8	7.4	13	15	12	15

measured with ECLIA (NSEαγ + NSEγγ) in 683 patients suspected of having lung cancer, with a median concentration of 62 ng/mL in the SCLC patients [25]. As the total NSE concentration is expected to be dominated by NSEγ which is present in both NSEαγ and NSEγγ, the detection ranges of both isozymes are expected to be sufficient for most of the SCLC patient samples.

The differences between the back–calculated concentrations of the isozyme calibration curves and the nominal values were used to calculate accuracy and precision, as shown in Table 2. The accuracy and precision levels of NSEγ were all < 20%, including the lowest calibration standard close to the LLoQ. For NSEα nearly all levels were < 20%, except for the mean accuracy at 19 ng/mL (34%) and the mean precision at 0.69 ng/mL (46%). For conventional ligand binding assays and chromatographic methods, the EMA guidelines describe tolerance levels < 20% and < 15% respectively, and < 25% and < 20% for the LLoQ. As yet, there are no guidelines for complex IA LC–MS/MS quantification assays of endogenous proteins, which contain more pretreatment steps including digestion. The described performances are therefore assumed to be acceptable, although a full–protein IS prior to sample purification is expected to lower variation.

No carry–over was observed for both the NSEα and NSEγ SP and their corresponding IS. Specificity towards NSEαγ and NSEγγ was confirmed, as no significant cross–reactivity towards αα enolase was observed when blank samples were compared to αα samples (<15%).

3.6. Detection in human serum samples

Nine independent human serum pools were used to test the applicability of the newly developed IA LC–MS/MS assay in patient samples. In addition, the NSE concentrations were quantified using a conventional ECLIA and the results were compared to IA LC–MS/MS (Fig. 4A). Both isozymes were successfully detected in all patient serum pools when using the IA LC-MS/MS assay, where all NSEγ concentrations were higher compared to NSEα. Comparison of the absolute concentrations quantified in both assays showed good correlation, although the total NSE concentration measured in IA LC–MS/MS was lower than in ECLIA with a mean bias of −122% (Fig. 4B). The reported concentrations are not directly interchangeable due to the different capturing antibody clones and potential interference components in ECLIA. This illustrates the need for extensive clinical validation before IA LC–MS/MS methodology is to be used in a clinical setting to allow interpretation of concentration differences and diagnostic cut-off values. To our knowledge, the true concentration of the individual NSE isozymes have never been established. The respective concentrations of NSE homo- and heterodimers therefore need to be studied in healthy subjects as well as SCLC patients. Such novel insights could also aid in improved hemolysis correction, as the predominant dimer in erythrocytes is NSEαγ, which is currently not discriminated from NSEγγ in ECLIA.

4. Conclusion

The combination of IA purification and LC–MS/MS quantification was, for the first time, shown to enable selective quantification of both NSEα and NSEγ isozymes in a multiplex format. Formation of NSEαγ heterodimers was achieved using cold denaturation, which induced reversible dissociation of the recombinantly expressed homodimers and provided a suitable calibrator containing both homo–and heterodimers. The IA LC–MS/MS assay provided sufficient LLoQs and showed correlation with the currently used immunoassay when measuring both NSE isozymes in patient serum. This multiplex IA LC–MS/MS assay sets the analytical foundation for NSE isozyme quantification that, after extensive clinical validation, may be a valuable tool to standardize immunological NSE assays and to obtain insights into the concentrations of NSE isozymes in patient cohorts. Potentially, this assay may better identify lung cancer compared to current immunoassays. Moreover, the multiplex IA LC–MS/MS assay has potential for the assessment of multiple lung cancer biomarkers in a more extended multiplex format, which requires different capturing antibodies and optimization of the isolation and LC–MS/MS parameters.

CRediT authorship contribution statement

Sylvia A.A.M. Genet: Conceptualization, Data curation, Formal analysis, Investigation, Methodology, Validation, Visualization, Writing – original draft. **Jur R.E. Wolfs:** Formal analysis, Investigation, Writing – review & editing. **Chris B.A.K. Vu:** Investigation, Writing – review & editing. **Madita Wolter:** Investigation, Writing – review & editing. **Maarten A.C. Broeren:** Conceptualization, Supervision, Validation, Writing – review & editing. **Joost van Dongen:** Conceptualization, Supervision, Validation, Writing – review & editing. **Luc Brunsveld:** Conceptualization, Funding acquisition, Resources, Supervision, Validation, Writing – review & editing. **Volkher Scharnhorst:** Conceptualization, Funding acquisition, Resources, Supervision, Validation, Writing – review & editing. **Daan van de Kerkhof:** Conceptualization, Supervision, Validation, Writing – review & editing.

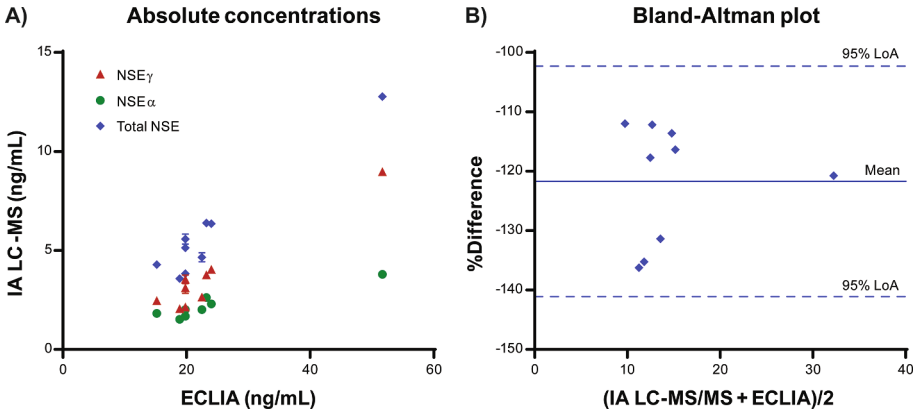

Fig. 4. Comparative study of the IA LC–MS/MS assay and ECLIA. A) Concentrations of NSEα (green dots), NSEγ (red triangles) and total NSE (NSEα + NSEγ, blue squares) in nine patient serum pools measured with the IA LC–MS/MS assay and ECLIA. B) The total NSE concentration (NSEα + NSEγ) quantified in IA LC–MS/MS compared to the total NSE concentration measured in ECLIA, showing significantly lower concentrations measured in IA LC–MS/MS compared to ECLIA with a mean bias of −122%. The y-axis of the Bland-Altman plot shows the %Difference: 100(IA LC-MS/MS – ECLIA) /average). ECLIA: electrochemiluminescent assay. (For interpretation of the references to colour in this figure legend, the reader is referred to the web version of this article.)

Funding

The study was supported by The Netherlands Organization for Scientific Research (NWO) with LIFT grant 731.017.405. Roche Diagnostics partially sponsored the NSE reagents used in this study. The funding organizations did not play a role in the study design, data interpretation or preparation of approval of the paper.

Declaration of Competing Interest

The authors declare the following financial interests/personal relationships which may be considered as potential competing interests: [Sylvia Genet reports financial support was provided by Nederlandse Organisatie voor Wetenschappelijk Onderzoek Utrecht.].

Data availability

Data will be made available on request.

Appendix A. Supplementary material

Supplementary data to this article can be found online at https://doi.org/10.1016/j.jchromb.2023.123701.

References

[1] B.W. Moore, D. McGregor, Chromatographic and Electrophoretic Fractionation of Soluble Proteins of Brain and Liver, J. Biol. Chem. 240 (1965) 1647–1653, https://doi.org/10.1016/S0021-9258(18)97483-1.
[2] F.J. Tapia, A.J.A. Barbosa, P.J. Marangos, J.M. Polak, S.R. Bloom, C. Dermody, A. G.E. Pearse, Neuron-specific enolase is produced by neuroendocrine tumours, The Lancet. 317 (1981) 808–811, https://doi.org/10.1016/S0140-6736(81)92682-9.
[3] T. Vizin, J. Kos, Gamma-enolase: a well-known tumour marker, with a less-known role in cancer, Radiol. Oncol. 49 (2015) 217–226, https://doi.org/10.1515/raon-2015-0035.
[4] M.A. Isgrò, P. Bottoni, R. Scatena, Neuron-Specific Enolase as a Biomarker: Biochemical and Clinical Aspects, Adv. Exp. Med. Biol. 867 (2015) 125–143, https://doi.org/10.1007/978-94-017-7215-0_9.
[5] V. Pancholi, Multifunctional α-enolase: its role in diseases, Cell. Mol. Life Sci. CMLS. 58 (2001) 902–920, https://doi.org/10.1007/PL00000910.
[6] D. Carney, D. Ihde, M. Cohen, P. Marangos, P. Bunn, J. Minna, A. Gazdar, Serum Neuron-Specific Enolase: a marker for disease extent and response to therapy of small-cell lung cancer, The Lancet. 319 (1982) 583–585, https://doi.org/10.1016/S0140-6736(82)91748-2.
[7] P.J. Marangos, I.C. Campbell, D.E. Schmechel, D.L. Murphy, F.K. Goodwin, Blood Platelets Contain a Neuron-Specific Enolase Subunit, J. Neurochem. 34 (1980) 1254–1258, https://doi.org/10.1111/j.1471-4159.1980.tb09967.x.
[8] D. Schmechel, P.J. Marangos, M. Brightman, Neurone-specific enolase is a molecular marker for peripheral and central neuroendocrine cells, Nature. 276 (1978) 834–836, https://doi.org/10.1038/276834a0.
[9] R. Molina, R.M. Marrades, J.M. Augé, J.M. Escudero, N. Viñolas, N. Reguart, J. Ramirez, X. Filella, L. Molins, A. Agustí, Assessment of a Combined Panel of Six Serum Tumor Markers for Lung Cancer, Am. J. Respir. Crit. Care Med. 193 (2015) 427–437, https://doi.org/10.1164/rccm.201404-0603OC.
[10] J.A. Bonner, J.A. Sloan, K.M. Rowland, G.G. Klee, J.W. Kugler, J.A. Mailliard, M. Wiesenfeld, J.E. Krook, A.W. Maksymiuk, E.G. Shaw, R.S. Marks, E.A. Perez, Significance of Neuron-specific Enolase Levels before and during Therapy for Small Cell Lung Cancer, Clin. Cancer Res. 6 (2000) 597–601.
[11] T. Zamay, G. Zamay, O. Kolovskaya, R. Zukov, M. Petrova, A. Gargaun, M. Berezovski, A. Kichkailo, T.N. Zamay, G.S. Zamay, O.S. Kolovskaya, R.A. Zukov, M.M. Petrova, A. Gargaun, M.V. Berezovski, A.S. Kichkailo, Current and Prospective Protein Biomarkers of Lung Cancer, Cancers. 9 (2017) 155, https://doi.org/10.3390/cancers9110155.
[12] R. Molina, S. Holdenrieder, J.M. Auge, A. Schalhorn, R. Hatz, P. Stieber, Diagnostic relevance of circulating biomarkers in patients with lung cancer, Cancer Biomark. 6 (2010) 163–178, https://doi.org/10.3233/CBM-2009-0127.
[13] E. Paus, T. Risberg, Establishment and Evaluation of a Radioimmunoassay for Neuron-Specific Enolase, Tumor Biol. 10 (1989) 23–30, https://doi.org/10.1159/000217590.
[14] P. Stern, V. Bartos, J. Uhrova, D. Bezdickova, Z. Vanickova, V. Tichy, K. Pelinkova, R. Prusa, T. Zima, Performance Characteristics of Seven Neuron-Specific Enolase Assays, Tumor Biol. 28 (2007) 84–92, https://doi.org/10.1159/000098441.
[15] K. Sorensen, U. Brodbeck, E. Paus, B. Norgaard-pedersen, An enzyme antigen immunoassay for the determination of neuron-specific enolase in serum samples, Clin. Chim. Acta. 175 (1988) 337–343, https://doi.org/10.1016/0009-8981(88)90111-8.
[16] S.A.A.M. Genet, E. Visser, B.E.E.M. van den Borne, M.-Y.-E. Soud, H.N. A. Belderbos, G. Stege, M.E.A. de Saegher, F. Eduati, M.A.C. Broeren, J. van Dongen, L. Brunsveld, D. van de Kerkhof, V. Scharnhorst, Correction of the NSE concentration in hemolyzed serum samples improves its diagnostic accuracy in small-cell lung cancer, Oncotarget. 11 (2020) 2660–2668, https://doi.org/10.18632/oncotarget.27664.
[17] H. Neubert, C.M. Shuford, T.V. Olah, F. Garofolo, G.A. Schultz, B.R. Jones, L. Amaravadi, O.F. Laterza, K. Xu, B.L. Ackermann, Protein Biomarker Quantification by Immunoaffinity Liquid Chromatography-Tandem Mass Spectrometry: Current State and Future Vision, Clin. Chem. 66 (2020) 282–301, https://doi.org/10.1093/clinchem/hvz022.
[18] A.N. Hoofnagle, J.O. Becker, M.H. Wener, J.W. Heinecke, Quantification of Thyroglobulin, a Low-Abundance Serum Protein, by Immunoaffinity Peptide Enrichment and Tandem Mass Spectrometry, Clin. Chem. 54 (2008) 1796–1804, https://doi.org/10.1373/clinchem.2008.109652.
[19] M.M. Kushnir, A.L. Rockwood, F.G. Strathmann, E.L. Frank, J.A. Straseski, A. W. Meikle, LC-MS/MS Measurement of Parathyroid Hormone-Related Peptide, Clin. Chem. 62 (2016) 218–226, https://doi.org/10.1373/clinchem.2015.244012.
[20] Y.-T. Chen, L.-P. Tuan, H.-W. Chen, I.-A. Wei, M.-Y. Chou, H.-M. Chen, Y.-C. Tyan, S.-F. Chen, Quantitative Analysis of Prostate Specific Antigen Isoforms Using Immunoprecipitation and Stable Isotope Labeling Mass Spectrometry, Anal. Chem. 87 (2015) 545–553, https://doi.org/10.1021/ac5033066.
[21] S.B. Torsetnes, S.G. Løvbak, C. Claus, H. Lund, M.S. Nordlund, E. Paus, T. G. Halvorsen, L. Reubsaet, Immunocapture and LC–MS/MS for selective quantification and differentiation of the isozymes of the biomarker neuron-specific enolase in serum, J. Chromatogr. B. 929 (2013) 125–132, https://doi.org/10.1016/j.jchromb.2013.04.010.
[22] S.B. Torsetnes, M.S. Levernæs, M.N. Broughton, E. Paus, T.G. Halvorsen, L. Reubsaet, Multiplexing Determination of Small Cell Lung Cancer Biomarkers and Their Isovariants in Serum by Immunocapture LC-MS/MS, Anal. Chem. 86 (2014) 6983–6992, https://doi.org/10.1021/ac500986t.
[23] E. Visser, R. de Kock, S. Genet, B. van den Borne, M.-Y.-E. Soud, H. Belderbos, G. Stege, M. de Saegher, S. van 't Westeinde, M. Broeren, F. Eduati, B. Deiman, V. Scharnhorst, Up-front mutation detection in circulating tumor DNA by droplet digital PCR has added diagnostic value in lung cancer, Transl. Oncol. 27 (2023), 101589, https://doi.org/10.1016/j.tranon.2022.101589.
[24] R. de Kock, B. van den Borne, M.-Y.-E. Soud, H. Belderbos, G. Stege, M. de Saegher, C. van Dongen-Schrover, S. Genet, L. Brunsveld, V. Scharnhorst, B. Deiman, Circulating biomarkers for monitoring therapy response and detection of disease progression in lung cancer patients, Cancer Treat. Res. Commun. 28 (2021), 100410, https://doi.org/10.1016/j.ctarc.2021.100410.
[25] E. Visser, S. Genet, R. de Kock, B. van den Borne, M.Y.-E. Soud, H. Belderbos, G. Stege, M. de Saegher, S. van 't Westeinde, L. Brunsveld, M. Broeren, D. van de Kerkhof, B. Deiman, F. Eduati, V. Scharnhorst, Liquid biopsy-based decision support algorithms for diagnosis and subtyping of lung cancer, Lung Cancer. (Under submission).
[26] E. Paus, K. Hirzel, M. Lidqvist, M. Höyhtyä, D.J. Warren, TD-12 workshop report: characterization of monoclonal antibodies to neuron-specific enolase, Tumor Biol. 32 (2011) 819–829, https://doi.org/10.1007/s13277-011-0184-3.
[27] G.A.O. Cremers, B.J.H.M. Rosier, R. Riera Brillas, L. Albertazzi, T.F.A. de Greef, Efficient Small-Scale Conjugation of DNA to Primary Antibodies for Multiplexed Cellular Targeting, Bioconjug. Chem. 30 (2019) 2384–2392, https://doi.org/10.1021/acs.bioconjchem.9b00490.
[28] M. Dubois, F. Becher, A. Herbet, E. Ezan, Immuno-mass spectrometry assay of EPI-HNE4, a recombinant protein inhibitor of human elastase, Rapid Commun. Mass Spectrom. 21 (2007) 352–358, https://doi.org/10.1002/rcm.2844.
[29] R.A. Wevers, A.A.C. Jacobs, O.R. Hommes, A bioluminescent assay for enolase (EC 4.2.1.11) activity in human serum and cerebrospinal fluid, Clin. Chim. Acta. 135 (1983) 159–168, https://doi.org/10.1016/0009-8981(83)90131-6.
[30] J.A. Kornblatt, M.J. Kornblatt, G.H.B. Hoa, Second derivative spectroscopy of enolase at high hydrostatic pressure: An approach to the study of macromolecular interactions, Biochemistry. 34 (1995) 1218–1223, https://doi.org/10.1021/bi00004a015.
[31] G. Chai, J.M. Brewer, L.L. Lovelace, T. Aoki, W. Minor, L. Lebioda, Expression, Purification and the 1.8Å Resolution Crystal Structure of Human Neuron Specific Enolase, J. Mol. Biol. 341 (2004) 1015–1021, https://doi.org/10.1016/j.jmb.2004.05.068.
[32] P.L. Privalov, Cold Denaturation of Protein, Crit. Rev. Biochem. Mol. Biol. 25 (1990) 281–306, https://doi.org/10.3109/10409239009090612.
[33] S. Kunugi, N. Tanaka, Cold denaturation of proteins under high pressure, Biochim. Biophys. Acta BBA - Protein Struct Mol. Enzymol. 1595 (2002) 329–344, https://doi.org/10.1016/S0167-4838(01)00354-5.
[34] M. Jaremko, Ł. Jaremko, H.-Y. Kim, M.-K. Cho, C.D. Schwieters, K. Giller, S. Becker, M. Zweckstetter, Cold denaturation of a protein dimer monitored at atomic resolution, Nat. Chem. Biol. 9 (2013) 264–270, https://doi.org/10.1038/nchembio.1181.